IEEE Access
Multidisciplinary | Rapid Review | Open Access Journal

Received September 24, 2021, accepted October 24, 2021, date of publication November 2, 2021,
date of current version November 11, 2021.

Digital Object Identifier 10.1109/ACCESS.2021.3124905

High-Efficiency FCME-Based Noise Power Estimation for Long-Term and Wide-Band Spectrum Measurements

HIROKI IWATA[1], (Member, IEEE), KENTA UMEBAYASHI[1], (Member, IEEE), AHMED AL-TAHMEESSCHI[1], (Member, IEEE), AND JANNE LEHTOMÄKI[2], (Member, IEEE)

[1]Graduate School of Engineering, Tokyo University of Agriculture and Technology, Koganei 184-8588, Japan
[2]Centre for Wireless Communications, University of Oulu, 90014 Oulu, Finland

Corresponding author: Hiroki Iwata (hiroki_iwata@ieee.org)

This work was supported in part by the European Commission in the framework of the H2020-EUJ-02-2018 project 5GEnhance under Grant 815056, in part by the "Strategic Information and Communications R&D Promotion Programme (SCOPE)" of Ministry of Internal Affairs and Communications (MIC) of Japan under Grant JPJ000595, in part by the Japan Society for the Promotion of Science (JSPS) KAKENHI under Grant JP18K04124 and Grant JP18KK0109, and in part by the Institute of Global Innovation Research in Tokyo University of Agriculture and Technology. The work of Janne Lehtomäki was supported by the Academy of Finland 6Genesis Flagship under Grant 318927, and in part by the Infotech Oulu.

ABSTRACT Statistics in terms of spectrum occupancy are useful for efficient and smart dynamic spectrum sharing, and the statistics can be obtained by long-term and wide-band spectrum measurements. In this paper, we investigate noise floor (NF) estimation for energy detection (ED)-based long-term and wide-band spectrum measurements since the NF estimation heavily affects the ED performance and eventually the accuracy of the statistics in terms of spectrum occupancy. Specifically, we address the following NF estimation problems simultaneously for the first time in the spectrum measurement field: (1) *slow* time-varying property of the NF, (2) frequency dependency of the NF, (3) the NF estimation in the presence of the signal, and (4) the computational cost of the NF estimation. Firstly, we apply Forward consecutive mean excision (FCME) algorithm-based NF estimation to deal with the above three problems ((1), (2) and (3)) successfully. Second, we propose and apply an NF level change detection on top of the FCME algorithm-based NF estimation to deal with the fourth problem. The proposed NF level change detection exploits the *slow* time-varying property of the NF. Specifically, only if the significant NF level change is detected, the FCME algorithm-based NF estimation is performed to reduce the redundant NF estimations. In numerical evaluations, we show the efficiency and the validity of the NF level change detection for the NF estimation problems, and compare the NF estimation performance with the method without the NF level change detection.

INDEX TERMS Noise floor estimation, energy detection, dynamic spectrum access, spectrum measurement.

I. INTRODUCTION

During the past decades, the demand for radio spectrum has been increasing to support the bandwidth-hungry applications such as high-definition video streaming and emerging applications (e.g., Internet of things (IoT), device-to-device (D2D) communications), while there is little room to accommodate new emerging wireless systems due mainly to fixed spectrum assignment policy. However, the spectrum measurement campaigns around the world have shown that almost all the spectrum is under-utilized in time and/or space domains [2], [3]. It means there are a lot of unused spectrum called white space (WS). In order to solve this issue, several types of dynamic spectrum sharing (DSS) frameworks have been investigated, such as opportunistic spectrum access (OSA) [4], licensed shared access (LSA) in Europe [5], and television white space (TVWS) [6], citizens broadband radio service (CBRS) based on spectrum access system in the U.S. [7].

In typical OSA, there are primary users (PUs), which have priority regarding spectrum usage, and secondary users (SUs), which can opportunistically access the WS as long as

The associate editor coordinating the review of this manuscript and approving it for publication was Shuangqing Wei.

the spectrum utilization by SUs does not cause any harmful interference to PUs. OSA includes two important techniques: spectrum sensing and wireless resource management (e.g., bandwidth, power, etc.). Spectrum sensing is a spectrum awareness technique in terms of instantaneous spectrum occupancy, either vacant or occupied [8]. The requirements of spectrum sensing, such as accuracy, latency, and implementation cost are substantially demanding [9]. On the other hand, in the wireless resource management in the context of DSS, it is required to manage wireless resources to enhance the spectrum utilization efficiency while SUs do not cause any harmful interference to PUs.

In order to resolve the issue of spectrum sensing and provide an efficient wireless resource management, the advanced DSA approach (known as smart spectrum access (SSA)) has been investigated [10], [11]. In SSA, the aspect of spectrum usage by PU, such as statistics of channel occupancy rate (COR), which is the fraction of the time that a channel is occupied, i.e., contains signal(s) in addition to noise [12], can be available based on long-term, wide-band, and wide area spectrum measurements [13]. In fact, COR statistics can enhance not only spectrum sensing performance [14], [15], but also the efficiency of spectrum management, channel selection and MAC protocol [16], [17].

In this paper, we focus on the spectrum measurement part for realizing SSA. In general, the spectrum measurement consists of the acquisition of data associated with spectrum usage (e.g., I/Q data, power data) and processing the obtained data such as spectrum analysis, spectrum usage detection, and estimation of statistical information such as COR. Actually, there have been many spectrum measurement campaigns (see [2], [3] and references therein), and most of the campaigns use an energy detector (ED) as a spectrum usage detection technique. We also focus on the ED-based spectrum measurements.

One key challenge for the ED is the detection threshold-setting to achieve target detection performances, such as target false alarm rate. Therefore, there are several threshold setting criteria including the m-dB criterion and the constant false alarm rate (CFAR) criterion [18]. Basically, we need an accurate noise floor (NF) information no matter what criteria we adopt to set the threshold satisfying an adopted criterion. Actually, importance of the accurate NF estimation has been pointed out [19] since the inaccurate NF information leads to the deviated detection performance (probabilities of detection and false alarm) from the target one, i.e., non-guaranteed detection performance. In addition, the inaccurate NF information also leads to Signal-to-Noise Ratio (SNR) wall phenomenon in ED [20].

Through our long-term and wide-band NF measurements and existing works [21]–[23], we have identified the following challenging problems for the NF estimation: (1) slow time-varying property of the NF, (2) frequency dependency of the NF, (3) the NF estimation in the presence of the signal. In addition, (4) the computational cost of the NF estimation needs to be considered since it is expected to deploy many low-cost spectrum sensors in the long-term, wide-band, and wide-area measurements.

Most of the previous spectrum measurements utilizing ED have assumed a static NF (time-invariant NF), which is obtained by switching the receiver input to a matched load or is measured in an anechoic chamber before starting the measurements [24]–[26]. Thus, these estimations do not take the problem (1) into account, while they can take the problem (2) into account partly. We note that the problem (3) is not an issue in these estimations since these estimations can exclude the target wireless system signal. Obviously, these estimations also have the low computational complexity since the NF estimation is done only once. In this paper, we refer to the NF estimation that estimates the NF once before starting the measurements as the static estimation method.

On the other hand, some existing works take the problems (1) and (2) into account. The typical related works in the spectrum usage measurement field and the cognitive radio field include [27]–[33] as far as we know. These works can address the problem (1) by successive NF estimations between consecutive measurements (say, 1 second interval). In addition, they can also address the problem (3) by morphological image processing operations [27], rank-order filtering (ROF) [28], [29], Gaussian mixture model [30], auto-correlation estimation [31] or Forward consecutive mean excision (FCME) algorithm [32], [33]. The reference [27] also addresses the third problem as well as the second problem.

Especially, the FCME algorithm-based NF estimation is based on the signal detection theory [34]. Specifically, it classifies the measured signal into two group (signal group and noise group) and calculates the arithmetic mean of the noise group resulting to the NF estimate. However, the original FCME algorithm-based NF estimation does not take the third problem directly into account. In response to the disadvantage of the FCME algorithm-based NF estimation, the two dimensional FCME algorithm-based NF estimation was presented in a conference paper [23]. The method can take the problems (1)-(3) into account at the same time and it is the state-of-the-art NF estimation method according to our best knowledge. However, the problem (4) has not been addressed (i.e., heavy computational complexity) since the method must do the NF estimation frequently while the actual NF varies with time slowly [21]. Namely, frequent NF estimations lead to the excessive computational cost (estimation run-time) for NF estimation.

Therefore, this paper proposes and applies an NF level change detection for the efficient NF estimation based on FCME algorithm.[1] Specifically, the NF estimation is performed only when a significant NF level change is detected. Our aim is to reduce the run-time for the NF estimation process as much as possible while achieving the comparable NF estimation performance with respect to the state-of-

[1] In comparison to our conference paper [1], new contributions in this paper are design of hyperparameters in the proposed NF estimation method, and optimal hyperparameters are shown. Extensive and thorough numerical evaluations present their validity.

the-art method and getting the obtained false alarm as close as possible to the target false alarm rate via the NF level change detection. The main contributions of this paper are as follows:

- We propose an NF level change detection method to decide whether the NF estimation can be skipped or not. The method is based on the ED result with detection threshold based on previous NF estimate. Thus, the NF estimation process is skipped when the previous detection threshold is decided to be adequate.
- The proposed method has the lower computational cost (run-time) of the NF estimation while it offers the comparable NF estimation performance with respect to the existing state-of-the-art two-dimensional FCME algorithm-based NF estimation method. In addition, the proposed method has a better NF estimation performance than that of the static estimation method. We numerically verify them.

The rest of the paper is organized as follows: Section II is devoted to the description of spectrum usage measurement methodology, the time variation model of NF level and the significance of our work. In Section III, we introduce our proposed NF estimation process with the NF level change detection. The numerical evaluation and its corresponding discussion are provided in Section IV. Finally, Section V concludes our paper.

II. SYSTEM MODEL

A configuration of time frames for a spectrum measurement is shown in Fig. 1. The measurement period is set to long term, such as dozens of days. A spectrum sensor continuously acquires N complex baseband samples for one data acquisition period with the specified measurement bandwidth and accumulates them into its own local storage by the next data acquisition start. Data acquisition period is indexed with t, $t \in \{0, 1, \cdots, T-1\}$ and T indicates the total number of measurement.

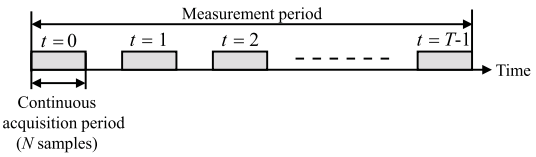

FIGURE 1. The configuration of time frames in measurement process.

The general signal processing used for the spectrum measurement is shown in Fig. 2. The first step is the power spectrum estimation with Welch FFT [35] using the baseband samples at the tth period $\mathbf{y}_t \in \mathbb{C}^N$. Then, the NF estimation is performed and we denote the estimated NF as $\hat{\mathbf{U}}_t \in \mathbb{R}^{N_{FFT}}$, where N_{FFT} is the FFT size exploited in Welch FFT and typically $N_{FFT} < N$ in Welch FFT. In the conventional approach, the NF estimation is performed every acquisition period. On the other hand, in our approach, the NF estimation is performed at tth acquisition period

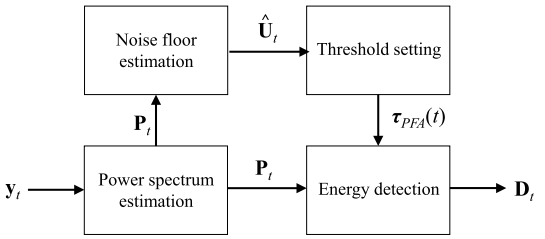

FIGURE 2. General signal processing model for spectrum measurement.

if a significant NF level change is detected. Otherwise the NF estimation at $t-1$th acquisition period is used in tth acquisition period. In Sect. III, the proposed NF estimation with the NF level change detection will be shown. After the NF estimation, the threshold setting for ED is performed with using $\hat{\mathbf{U}}_t$ based on the CFAR criterion. Finally, the ED with the set threshold $\boldsymbol{\tau}_{P_{FA}}(t)$ is performed to obtain the spectrum usage decisions $\mathbf{D}_t$. Below is the more detailed explanation for the process.

In the tth acquisition period, we model the baseband I/Q signal $\mathbf{y}_t = [y_t[0], y_t[1], \cdots, y_t[N-1]]^T \in \mathbb{C}^N$ as the complex Gaussian random signal since we focus on the broadband wireless system such as WLAN system and LTE system and most all the modern broadband wireless systems now apply the OFDM technology, where the OFDM signal can be approximated to the Gaussian random signal as indicated in [36] and [37]. However, the idea in the paper can be applied to any broadband wireless systems since the detection method (ED) and the proposed NF estimation method exploit power information that can be calculated for any radio signals. Thus, the sampled baseband signal bandlimited to the measurement bandwidth is given by

$$y_t[n] = \begin{cases} s_t[n] + z_t[n] & (\mathcal{H}_1) \\ z_t[n] & (\mathcal{H}_0), \end{cases} \tag{1}$$

where $s_t[n]$ and $z_t[n]$ are the nth observation target signal sample and the noise signal sample which are the complex Gaussian random signal with zero mean and variance $\sigma_s^2[t]$ or $\sigma_z^2[t]$, respectively. Moreover, the noise signal has a specific power spectrum shape (e.g., Fig. 3 (b)), but we assume that the target signal has a flat power spectrum over the measurement bandwidth. $\sigma_s^2[t]$ and $\sigma_z^2[t]$ are the signal power and the time-varying noise power at the tth acquisition period, respectively and we assume that these parameters are at least constant over one acquisition period. We define $SNR = \sigma_s^2[t]/\sigma_z^2[t]$ as the constant signal-to-noise ratio for the evaluation purpose in the numerical evaluation section. Thus, the total signal power is adjusted according to the given SNR value and the given total noise power at the tth acquisition period, i.e., $\sigma_s^2[t] = SNR \times \sigma_z^2[t]$. Moreover, the status $(\mathcal{H}_1)$ indicates that PU signal exists in the measurement bandwidth partially or completely and the status $(\mathcal{H}_0)$ indicates otherwise (no signal present).

At first, the baseband signal $\mathbf{y}_t$ is divided into K Welch FFT blocks with N_s samples. Thus, $\mathbf{y}_k^{(t)}$, $k \in \{0, 1, \cdots, K-1\}$

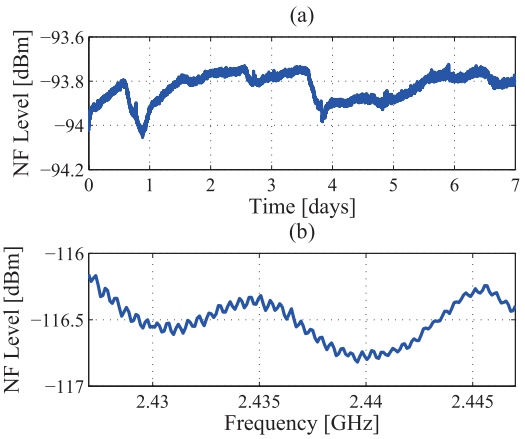

FIGURE 3. NF measurement ((a) NF level evolution, (b) Power spectrum of NF at 200kHz resolution bandwidth).

in the kth Welch FFT block is given by $\mathbf{y}_k^{(t)} = [y_t[kN_s], \cdots, y_t[kN_s + N_s - 1]]^T$. The power spectrum estimation with Welch FFT consists of three steps: segmentation of $\mathbf{y}_k^{(t)}$ with a specific FFT size and an overlap ratio, calculation of multiple power spectra, and averaging of the power spectra [35]. The baseband signal $\mathbf{y}_{k,l}^{(t)}$, $l \in \{0, 1, \cdots, L-1\}$ at lth segment and kth Welch FFT block is given by

$$\mathbf{y}_{k,l}^{(t)} = [y_t[kl(1-\rho)N_{FFT}], \cdots, y_t[kl(1-\rho)N_{FFT} + N_{FFT} - 1]]^T. \quad (2)$$

where N_{FFT} is the FFT size and the overlap ratio ρ is set to 0.5 [38]. Moreover, N_s and N_{FFT} are assumed to be powers of two. In this case, the number of segments L is given by $L = 2N_s/N_{FFT} - 1$.

After the segmentation, normal FFT is performed for each segment. The result of FFT operation of $\mathbf{y}_{k,l}^{(t)}$ is given by

$$\mathbf{Y}_{k,l}^{(t)} = \frac{1}{\sqrt{N_{FFT}}}\mathbf{F}\mathbf{W}\mathbf{y}_{k,l}^{(t)}, \quad (3)$$

where $\mathbf{F} = (exp(-j2\pi mf/N_{FFT}))_{m,f\in 0,1,\cdots,N_{FFT}-1}$ is the discrete Fourier transform matrix. The diagonal matrix $\mathbf{W} = diag(w_0, w_1, \cdots, w_{N_{FFT}-1})$ is a matrix where its diagonal elements are coefficients w_m of the utilized FFT window with $\sum_{m=0}^{N_{FFT}-1} w_m^2 = 1$. Hamming window is used in this process [33].

The calculated power spectra based on Welch FFT at kth Welch FFT block is given by

$$\mathbf{P}_k^{(t)} = \frac{1}{L}\sum_{l=0}^{L-1}|Y_{k,l}^{(t)}[f]|^2 = [P_k^{(t)}[0], \cdots, P_k^{(t)}[f], \cdots, P_k^{(t)}[N_{FFT}-1]]^T, \quad (4)$$

where $f \in \{0, 1, \cdots, N_{FFT} - 1\}$ indicates the index number of frequency bin. We define a matrix $\mathbf{P}_t = [\mathbf{P}_1^{(t)}\mathbf{P}_2^{(t)}\cdots\mathbf{P}_K^{(t)}] \in \mathbb{R}^{N_{FFT}\times K}$.

The ED result indicates a presence of signal component at the kth Welch FFT block and the fth frequency bin as

$$D_t[k,f] = \begin{cases} 1 & (P_k^{(t)}[f] > \tau_{P_{FA}}[f](t)) \\ 0 & (otherwise), \end{cases} \quad (5)$$

where 1 and 0 respectively indicate that a presence of signal component ($\mathcal{H}_1$) and an absence of signal component ($\mathcal{H}_0$) are assumed. The detection threshold $\boldsymbol{\tau}_{P_{FA}}(t)$ is set based on NF estimate $\hat{\boldsymbol{\Theta}}_t = [\hat{U}[t,0], \hat{U}[t,1], \cdots, \hat{U}[t,f], \cdots, \hat{U}[t,N_{FFT}-1]]^T$ so that $\tau_{P_{FA}}[f](t)$ satisfies the CFAR criterion.

A. TIME VARIATION MODEL OF NOISE FLOOR LEVEL

Fig. 3 shows (a) the time variation of the NF level for one week (01/12/2018–07/12/2018) and (b) the power spectrum of the NF. This result was measured at our laboratory in Koganei campus, Tokyo University of Agriculture and Technology, Tokyo, Japan. The spectrum sensor used was a real-time spectrum analyzer (Tektronix RSA306B). The result was obtained every one minute by switching the sensor input to a matched load. Fig. 3 (a) verifies that the NF level slowly changes with time between around −94.05dBm and −93.72dBm. On the other hand, Fig. 3 (b) shows that the NF has the frequency-dependency.

Based on our two dimensional NF measurement campaign, we model the NF level variation in time and frequency domains as [23]

$$U[j,f] = \gamma_j \mu_{ref}[f], \quad (6)$$

where γ_j and $\mu_{ref}[f]$ indicate the NF level variation factor and the NF at a reference time instant $j = t_{ref}$ denoted by the reference NF level, respectively. The coefficient γ_j indicates a gain to obtain the NF level at time j and it is frequency-independent. The reference NF level at a reference time can be obtained from a measurement in an anechoic chamber or by using a radio frequency (RF) terminator at the spectrum sensor to avoid the presence of signal component. Then, the reference NF $\mu_{ref}[f]$ is calculated by time averaging of noise power spectra, and it is given by

$$\mu_{ref}[f] = \frac{1}{M}\sum_{m=0}^{M-1} P_{m,ref}[f], \quad (7)$$

where M and $P_{m,ref}[f]$ indicate the number of time averaging and noise power spectrum, respectively. Furthermore, we assume the NF at least do not change during one data acquisition time.

B. SIGNIFICANCE OF NF LEVEL CHANGE

According to the result in Fig. 3 (a), the NF level change is at most 0.4 dB. This NF level change affects the obtained false alarm rate since estimated NF level is used to set the threshold $\tau_{P_{FA}}[f](t)$. The obtained false alarm rate can be calculated as follows [23]

$$P_{FA} = Prob(P_k^{(t)}[f] > \tau_{P_{FA}}|\mathcal{H}_0) = \tilde{\Gamma}\left(L, \frac{\tau_{P_{FA}}}{\gamma_t \mu_{ref}[f]/L}\right), \quad (8)$$

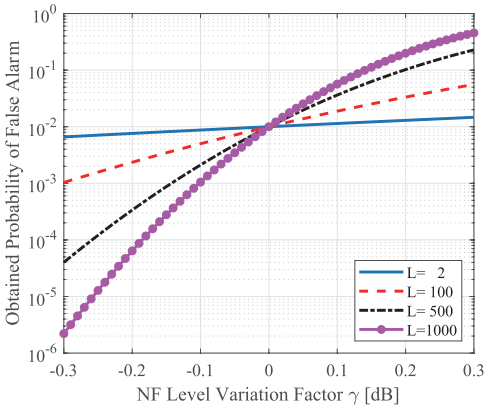

FIGURE 4. Obtained false alarm rate as a function of NF level variation factor.

where $\tilde{\Gamma}(\alpha, \theta)$ indicates a normalized incomplete Gamma function. The threshold $\tau_{P_{FA}}[f](t)$ is set based on the CFAR criterion and is given by [23]

$$\tau_{P_{FA}}[f] = \frac{\gamma \mu_{ref}[f]}{L} \tilde{\Gamma}^{-1}\left(L, \dot{P}_{FA}\right), \tag{9}$$

where $\dot{P}_{FA}$ is a given target false alarm rate and $\tilde{\Gamma}^{-1}$ indicates the inverse of a normalized incomplete Gamma function. Fig. 4 shows the obtained false alarm rate in case of the target false alarm rate $\dot{P}_{FA} = 0.01$ as a function of the NF level variation factor, γ, where γ implies the NF estimation error and $\gamma = 0$dB indicates no NF estimation error. The result indicates that the false alarm rate can be significantly large, such as 0.45 in the case of $L = 1000$ and $\gamma = 0.3$dB. This means the COR value may be estimated as 0.95 if the real COR value is 0.5 and measurement is in a high SNR environment. Therefore, the NF level change, such as $\gamma = 0.3$dB, is not negligible for false alarm rate. In addition, it is well know that this also leads to the SNR wall behaviour for energy detector [20].

III. PROPOSED NF ESTIMATION PROCESS

The block diagram of proposed NF estimation process is shown in Fig. 5. It consists of two blocks: Block 1 (B1), which is NF level change detection and Block 2 (B2), which is NF estimation based on the FCME algorithm. The process of NF level change detection in B1 is executed every data acquisition time t except for the first measurement $t = 0$. On the other hand, NF estimation in B2 is only executed when the NF level change is detected or $t = 0$ since the spectrum sensor does not know the NF at first. Therefore, the proposed method can reduce the computational cost of NF estimation processes if the computational cost of the process in B1 is smaller than one in B2 and the NF level changes slowly.

In B2, we exploit the two-dimensional FCME algorithm-based NF estimation as the NF estimation as it can achieve the highly-accurate NF estimation performance while considering the frequency-dependency of the NF [23]. Briefly, the two-dimensional FCME-based NF estimation estimates the NF level variation factor γ_t at time instant t exploiting the reference NF $\mu_{ref}[f]$ and the estimated power spectrum in the time-frequency plane $\mathbf{P}_t$, where the description of the reference NF is provided in Subsect. II-A [23]. More specifically, it locates the noise-only power samples in power spectrum samples $\mathbf{P}_t$ based on the FCME algorithm, flattens or normalizes the located noise-only power spectra in frequency exploiting $\mu_{ref}[f]$, and estimates γ_t by applying the FCME algorithm again. Then, the resultant NF estimate is $\hat{U}[t, f] = \hat{\gamma}_t \cdot \mu_{ref}[f]$ where $\hat{\gamma}_t$ indicates the estimate of γ_t. After estimating the NF in B2, the ED is performed based on the set threshold with the estimated NF.

On other hand, for other data acquisition time, i.e., $t \in \{1, 2, \cdots, T-1\}$, the processes in B1 are performed at first. It includes the tentative ED using the threshold from the previous data acquisition, i.e., $\tau_{P_{FA}}(t-1)$, and the NF level change detection. The frequency bins where detection decision was "noise-only" are used for noise level change detection. They are normalized using the reference NF and

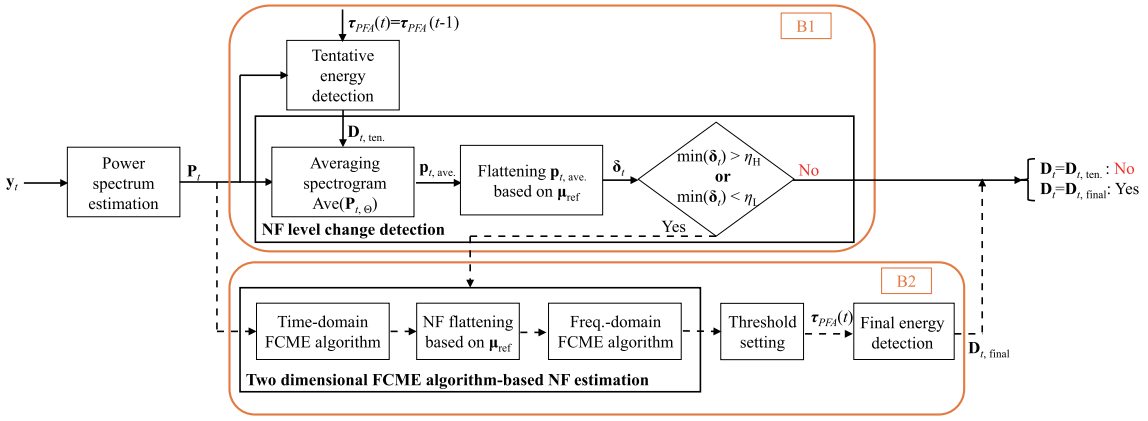

FIGURE 5. Block diagram of the proposed NF estimation process.

then minimum is taken. Minimum of ED decision values has been used for NF estimation [39] and here it is used for different purpose, for change detection. The normalized minimum is compared with two thresholds derived from the previous round NF level variation factor. The purpose is to notice when NF is increasing or decreasing. If the change of the NF is detected, the processes in B2 are enforced and the ED result is the final ED result, i.e., $\mathbf{D}_t = \mathbf{D}_{t,final}$. Otherwise, the ED result equals to the tentative ED result ($\mathbf{D}_t = \mathbf{D}_{t,ten.}$), and $\hat{U}[t,f] = \hat{U}[t-1,f]$ and $\tau_{P_{FA}}[f](t) = \tau_{P_{FA}}[f](t-1)$. Below is the more detailed description for the NF level change detection.

The NF level change detection exploits the result of the tentative ED, $\mathbf{D}_{t,ten.}$ and the power spectrum $\mathbf{P}_t$. Let a set $\Theta[f]$ to be a set consisting of the indices of zeros ("noise-only") in $\mathbf{D}_{t,ten.}[f]$, i.e., $\Theta[f] = \{k|\mathbf{D}_{t,ten.}[f] = 0\}$, where $\mathbf{D}_{t,ten.}[f]$ indicates the tentative ED result at frequency bin f. Then, we define a value $p_{t,ave.}[f]$ as the average value of a vector $\mathbf{p}_{t,\Theta}[f]$ in time. Specifically, $p_{t,ave.}[f]$ is given by

$$p_{t,ave.}[f] = \frac{1}{|\Theta[f]|} \sum_{k \in \Theta[f]} P_k^{(t)}[f], \tag{10}$$

where $|\Theta[f]|$ indicates the cardinality of $\Theta[f]$ and $\mathbf{p}_{t,\Theta}[f] = [P^{(t)}_{k\in\Theta[f]}[f]]$. After that, we perform the NF flattening process using the reference NF $\mu_{ref}[f]$. This process is done as

$$\delta_t[f] = \frac{p_{t,ave.}[f]}{\mu_{ref}[f]}. \tag{11}$$

We can detect the NF level change by the thresholding process against $\delta_t[f]$ since $\delta_t[f]$ can be an estimate of γ_t. Specifically, we decide that the NF level changes if $\min(\delta_t) > \eta_H$ or $\min(\delta_t) < \eta_L$. Otherwise, i.e., $\min(\delta_t)$ lies in between η_L and η_H, we decide that the NF level does not change. We apply two thresholds, η_L and η_H since the NF level possibly increases or decreases. Both thresholds are set based on $\hat{\gamma}_{t-1}$ and two hyperparameters (Δ_L, Δ_H) and these are given by

$$\eta_L = \Delta_L \cdot \hat{\gamma}_{t-1}, \eta_H = \Delta_H \cdot \hat{\gamma}_{t-1}, \tag{12}$$

where the hyperparameters are set in advance before the spectrum measurements by solving the following optimization problem 14 via the exhaustive search.

To set the hyperparameters properly, we introduce a min-max optimization problem as follows. It minimizes the maximum computational cost (run-time) in terms of NF estimation process over the whole target SNR region, while the mean absolute error (MAE) between the obtained false alarm rate $P_{FA,o}$ and the target false alarm rate $\dot{P}_{FA}$ is lower than the allowable mean absolute error. The MAE of the false alarm rate implies the NF estimation performance since the good NF estimation leads to the smaller MAE and is given by

$$\mathrm{MAE}_{P_{FA}}(\eta_L, \eta_H) = \mathbb{E}[|P_{FA,o} - \dot{P}_{FA}|], \tag{13}$$

where $\mathbb{E}[\cdot]$ denotes expectation. Mathematically, the above criterion is defined as

$$\min_{\{\eta_L,\eta_H\}} \max_{SNR\in[SNR_{min}\ SNR_{max}]} \mathrm{C}(\eta_L, \eta_H; SNR)$$
$$\text{subject to } \mathrm{MAE}_{P_{FA}}(\eta_L, \eta_H; SNR) \le \epsilon_{P_{FA}}, \tag{14}$$

where $\mathrm{C}(\eta_L, \eta_H; SNR)$, $\mathrm{MAE}_{P_{FA}}(\eta_L, \eta_H)$ and $\epsilon_{P_{FA}}$ indicate the run-time given an SNR and hyperparameters, the MAE in terms of the obtained false alarm rate given an SNR and hyperparameters, and the allowable MAE of false alarm rate, respectively. The target SNR region is between SNR_{min} and SNR_{max}, where SNR_{min} and SNR_{max} are the minimum target SNR value and the maximum target SNR value, respectively.

IV. NUMERICAL EVALUATIONS

In this section, we evaluate the NF estimation performance and the spectrum occupancy detection performance of the proposed method based on computer simulations. For comparison, we evaluate the performances of the widely used static estimation method and the two-dimensional FCME algorithm-based NF estimation [23] which is the current state-of-the-art method. We assume the spectrum measurements of one wireless local area network (WLAN) channel with 20MHz bandwidth over 2.4GHz band and there is no signal in adjacent channels except the target channel. Common parameters are summarized in Table 1. Fig. 6 shows (a) the assumed NF variation in time and (b) the assumed reference NF, respectively. These correspond to the approximation to the NF by noise measurements as mentioned in Subsec. II-A (Fig. 3). Specifically, we calculated the NF level and the power spectrum of the NF (the reference NF) according to the experimental result of Fig. 3 by means of polynomial approximation. All the results in this section are evaluated using the time variation pattern and the power spectrum of the NF as shown in Fig. 6.

TABLE 1. Parameter set.

Parameter name	Parameter
One acquisition period N	2×10^6
Welch FFT block size N_s	2^{11}
FFT size N_{FFT}	2^8
$N_{trial} = T$	10260
$\sigma_z^2[t=0]$	-94dBm
SNR [dB]	[-10 10]
Channel occupancy rate	0.2, 0.5 and 0.8
Measurement bandwidth	20MHz
Center frequency	2.437GHz
Signal bandwidth	20MHz
$\dot{P}_{FA}$	0.01
$\epsilon_{P_{FA}}$	0.002

A. HYPERPARAMETERS OPTIMIZATION

In this subsection, the hyperparameters, Δ_L and Δ_H, are optimized based on (14). We show the optimization result in the case of COR $= 0.5$ as an example. The target SNR region is set to $SNR \in [-10\ 10]$ in dB, $\epsilon_{P_{FA}} = 2\times10^{-3}$ and the target false alarm rate is set to 0.01. An exhaustive search is applied

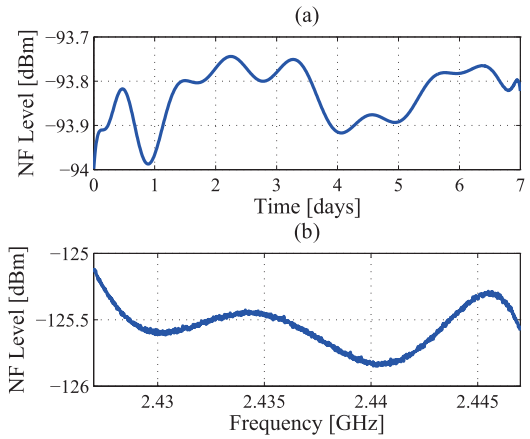

FIGURE 6. NF setting in the simulations ((a) Assumed NF evolution, (b) Assumed reference NF).

to find the optimal solution, i.e. $\Delta_L = 0.83$ and $\Delta_H = 0.91$. The search range is $\Delta_L = 0.75$ to $\Delta_L = 0.95$ and $\Delta_H = 0.75$ to $\Delta_H = 0.95$ with 0.01 step size. This leads to 210 possible combinations of the hyperparameters considering $\Delta_H > \Delta_L$. The obtained false alarm rate is defined by

$$P_{FA,o,t} = \frac{\sum_{f=0}^{N_{FFT}-1} \sum_{k=0}^{K-1} D_t[k,f]|\mathcal{H}_0}{N_{\mathcal{H}_0}}, \tag{15}$$

where $D_t[k,f]|\mathcal{H}_0$ and $N_{\mathcal{H}_0}$ are the detection result given the true $\mathcal{H}_0$ state and the total number of the true $\mathcal{H}_0$ state in the time and frequency domain, respectively.

To confirm the impact of Δ_L and Δ_H on performances, Figs. 7 and 8 show the MAE of false alarm rate and the average rum time which indicates the computational cost. Specifically, the performances obtained by the optimal solution and non-optimal cases are compared in the figures. The selected non-optimal Δ_L and Δ_H are ($\Delta_L = 0.87$ and $\Delta_H = 0.89$) and ($\Delta_L = 0.87$ and $\Delta_H = 0.93$). The former non-optimal case ($\Delta_L = 0.87$ and $\Delta_H = 0.89$) can achieve the lowest MAE performance in the target SNR region as

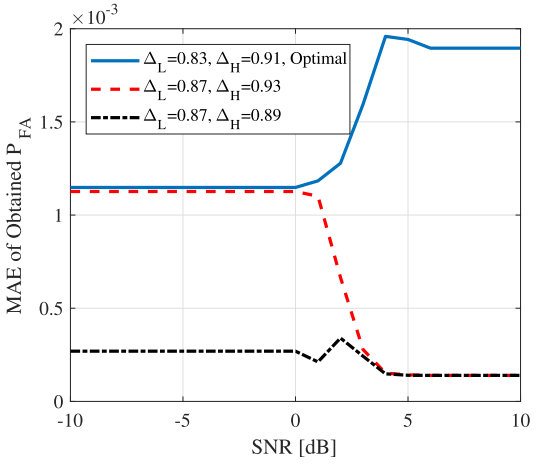

FIGURE 7. MAE in terms of the obtained P_{FA} as a function of *SNR*.

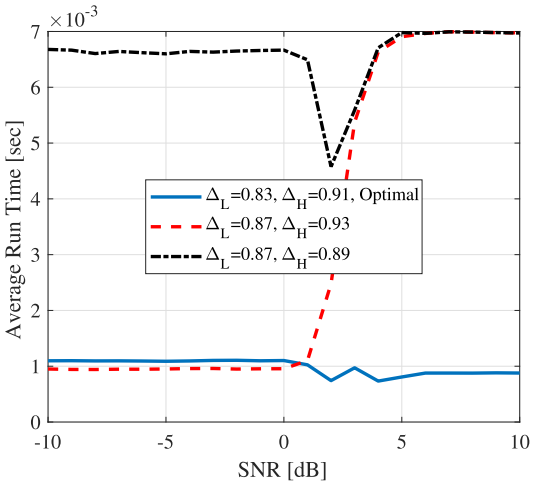

FIGURE 8. Average run time as a function of *SNR*.

shown in Fig. 7. However, the average run time in Fig. 8 is longest in the target SNR region. Thus, this result indicates the trade-off relationship between the run-time performance and the NF estimation accuracy for the proposed method and it is due to the NF level change detection. Thus, more skipping the NF estimation process, shorter the run-time, but worse the NF estimation performance and vice versa. However, we note that the MAE in terms of the obtained false alarm rate for the proposed method can satisfy the allowable MAE, $\epsilon_{P_{FA}}$.

The result in the later non-optimal case ($\Delta_L = 0.87$ and $\Delta_H = 0.93$) indicates an another trade-off in terms of the MAE of false alarm rate and the run-time performances as a function of SNR. Specifically, in the low SNR region, such as less than 1 dB, the MAE of false alarm rate is relatively high, but it is low in the high SNR region. On the other hand, in the low SNR region, the least run time is achievable, however it has the longer run time in the high SNR region. This implies that it is required to properly set the hyperparameters for the NF level change detection. Thus, the thresholds (or Δ_L and Δ_H) for the NF level change detection in the later non-optimal case are almost proper from the perspective of the hyperparameters optimization problem (14) since the MAE of the obtained false alarm rate and the average run time in the later non-optimal case are almost same as ones in the case of the optimal solution in the low SNR region. However, the thresholds in the later non-optimal case are not proper from the perspective of the computational cost (i.e., longer run time than one for the optimal solution) in the high SNR region since the upper threshold (i.e., $\Delta_H = 0.93$) for the later non-optimal case is slightly higher than the optimal upper threshold ($\Delta_H = 0.91$). In fact, the decision statistics of the NF level change detection (the minimum statistics of δ_t, $\min(\delta_t)$) tends to be larger as the SNR increases. As a result, the upper threshold for the later non-optimal case results in an increase in the number of the two-dimensional FCME algorithm-based NF estimation executed, i.e., longer run time in the high SNR region since the number that the NF level changes are detected increases.

B. COMPARATIVE EVALUATION

In this subsection, we compare performance of the proposed NF estimation and the two-dimensional FCME algorithm-based NF estimation when the COR is 0.2, 0.5 and 0.8 in the time-varying NF scenario. We use the time variation pattern of the NF as shown in Fig. 6 (a). The different COR values indicate the low, moderate, and high channel occupancy environments, respectively. For the proposed NF estimation, we use the optimal hyperparameters for each COR value found by the exhaustive search mentioned in the previous subsection. Thus, the optimal hyperparameters are $\Delta_L = 0.75$, $\Delta_H = 0.94$, $\Delta_L = 0.83$, $\Delta_H = 0.91$ and $\Delta_L = 0.82$, $\Delta_H = 0.90$ for $COR = 0.2$, 0.5 and 0.8, respectively.

Fig. 9 evaluates the NF estimation performance. Specifically, the figure shows the MAE in terms of the NF estimation and is defined as follow:

$$\mathrm{MAE}_{NF} = \frac{1}{T}\sum_{t=0}^{T-1}\sum_{f=0}^{N_{FFT}-1} |\hat{U}[t,f] - U[t,f]|, \qquad (16)$$

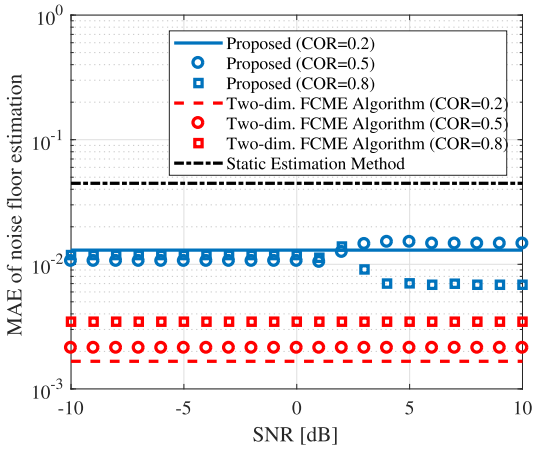

FIGURE 9. MAE in terms of the NF estimation in linear scale.

where T, N_{FFT} $\hat{U}[t,f]$ and $U[t,f]$ is the number of measurements (number of simulation trials), the number of frequency bins, the estimated NF in linear scale at tth measurement and fth frequency bin and the true NF in linear scale at tth measurement and fth frequency bin, respectively. For reference, the result of the static estimation method is also shown.

From this figure, the two-dimensional FCME algorithm-based NF estimation has a better NF estimation performance than the proposed method in the target SNR region since the proposed method can skip the two-dimensional FCME-based NF estimation by applying the NF level change detection to reduce the computational cost (run-time) at the cost of the slight NF estimation accuracy. Actually, it indicates the trade-off relationship between the computational cost and the NF estimation accuracy for the proposed method as mentioned in the previous subsection.

Moreover, for the two-dimensional FCME algorithm-based NF estimation, we can see the different NF estimation performance for each COR value. This is due to the less number of noise samples in the case of the higher COR value. In fact, the method in principle estimates the NF by averaging the noise samples.

On the other hand, we can see that both the proposed method and the two-dimensional FCME algorithm-based NF estimation have a much better NF estimation performance than one of the static estimation method. This is because that the static estimation method estimates the NF only once when starting the measurements and cannot track the time variation of the NF while both the proposed method and the two-dimensional FCME algorithm-based NF estimation can do it.

Figs. 10 and 11 show probabilities of detection and false alarm, respectively. For the probability of detection result, we only show the result in the case of $COR = 0.5$ since other probability of detection results for $COR = 0.2$ and $COR = 0.8$ are almost same as the result of $COR = 0.5$ and it is easy to see the result. From Fig. 10, we can see that both NF estimation methods attain the comparative detection

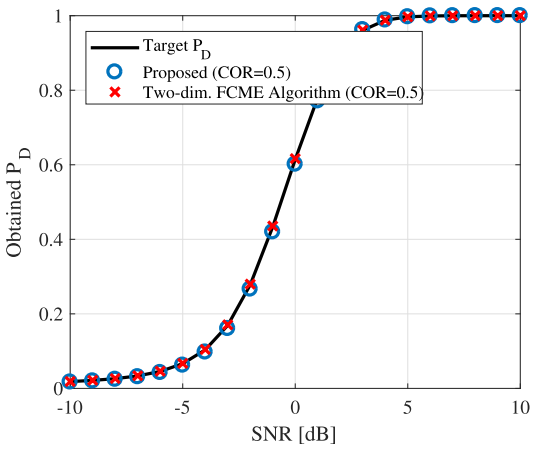

FIGURE 10. Probability of detection as a function of *SNR*.

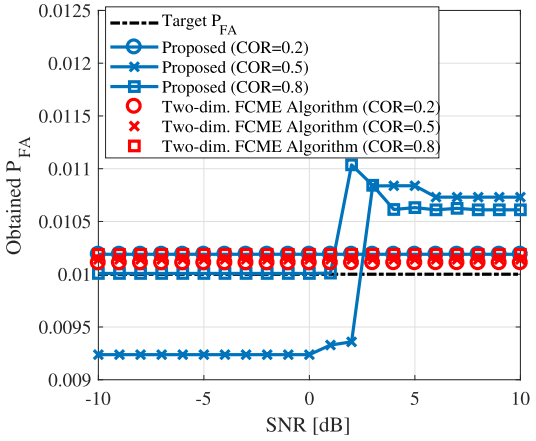

FIGURE 11. Probability of false alarm as a function of *SNR*.

probability and have a nearly equal detection probability to the ideal and target detection performance due to the highly accurate NF estimation. Here, the ideal and target detection probability indicates the probability of detection with the detection threshold (9) applying the 0.01 target false alarm rate.

On the other hand, Fig. 11 shows the small difference in terms of the obtained false alarm rate between the proposed method and the two-dimensional FCME algorithm-based NF estimation. This result is related to the NF estimation performance shown in Fig. 9. Thus, the lower MAE in terms of the NF estimation has the closer false alarm rate to the target false alarm rate with 0.01 and vice versa.

Fig. 12 shows the MAE in terms of the obtained false alarm rate of the proposed method and the two-dimensional FCME algorithm-based NF estimation. The figure indicates that both methods satisfy the allowable MAE accuracy, $\epsilon_{P_{FA}} = 0.002$. However, the two-dimensional FCME algorithm-based NF estimation has better MAE performance since the two-dimensional FCME algorithm-based NF estimation has better NF estimation performance as shown in Fig. 9. In fact, the result is related to the NF estimation performance shown in Fig. 9 due to (8). Thus, the lower MAE in terms of the NF estimation results in the lower MAE in terms of the false alarm rate and vice versa.

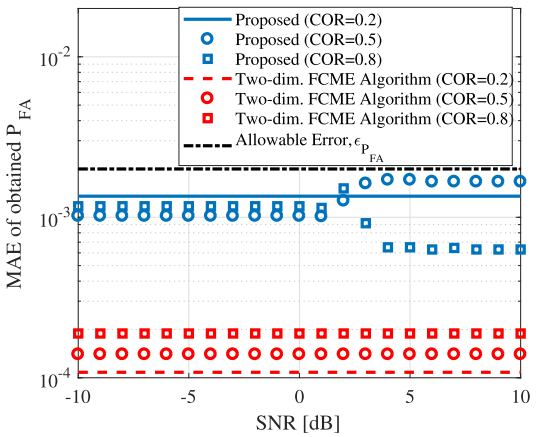

FIGURE 12. MAE in terms of the obtained P_{FA} as a function of SNR.

Finally, we evaluate the average run-time of the proposed method and the two-dimensional FCME algorithm-based NF estimation. Fig. 13 shows the run-time of the proposed method is at most 10 times faster than one of the two-dimensional FCME algorithm-based NF estimation in the case where $COR = 0.2$. On the other hand, the run-time of the proposed method is at most 2 times faster than the one of the two-dimensional FCME algorithm-based NF estimation in the case where $COR = 0.8$. Comparing with Fig. 12, we can see that these two figures are inter-related. In fact, the lower MAE of the obtained false alarm rate, the higher the average run time due to the trade-off between the NF estimation performance and the computational cost (run-time) for the proposed method. On the other hand, the average

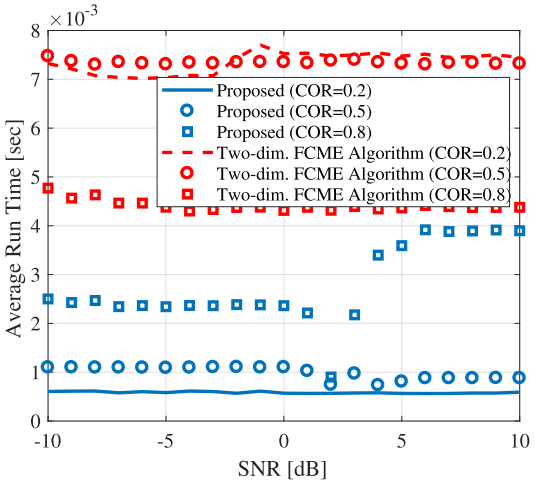

FIGURE 13. Computational cost (run-time).

run time of the two-dimensional FCME algorithm-based NF estimation is shorter in the case of the high COR value. This is due to the less number of noise samples averaging for the NF estimation. Therefore, the proposed approach can reduce the computational cost (run-time) significantly while maintaining accuracy of NF estimation.

V. CONCLUSION

In this paper, we have proposed an efficient NF estimation process (NF level change detection plus FCME algorithm-based NF estimation) for ED-based long-term and wide-band spectrum measurements. In fact, the proposed NF estimation process can deal with *slow* time-varying property and frequency dependency of the NF, the NF estimation in the presence of the signal, and the computational cost at the same time. Especially, the proposed process attempts to reduce the computational cost by exploiting *slow* time-varying NF via the proposed NF level change detection. Numerical evaluations have shown that the proposed method enables an accurate spectrum occupancy detection, considering the frequency-dependency and slowly time-varying property of the NF, while it can achieve 10 times faster run-time than one of the FCME algorithm-based NF estimation without the NF level change detection in case of the low COR environment. In this paper, we have numerically evaluated the effect of the thresholds on the NF estimation performance and the computational cost and shown the trade-off relationship between the NF estimation performance and the computational cost. As one of our future works, we will analyze the trade-off relationship theoretically. In addition, we will investigate a thresholds (hyperparameters) setting method for the proposed NF estimation method that satisfies the optimization problem (Eq. (14)).

ACKNOWLEDGMENT

This article was presented in part at the 2020 IEEE Wireless Communications and Networking Conference (WCNC) International Workshop on Smart Spectrum (IWSS 2020) [DOI: 10.1109/WCNCW48565.2020.9124906].

REFERENCES

[1] H. Iwata, K. Umebayashi, S. Joshi, A. Al-Tahmeesschi, M. López-Benítez, and J. Lehtomäki, "A study on high-efficiency energy detection-based spectrum measurements," in *Proc. IEEE Wireless Commun. Netw. Conf. Workshops (WCNCW)*, Apr. 2020, pp. 1–6.

[2] D. Das and S. Das, "A survey on spectrum occupancy measurement for cognitive radio," *Wireless Pers. Commun.*, vol. 85, no. 4, pp. 2581–2598, Dec. 2015.

[3] M. Höyhtyä, A. Mämmelä, M. Eskola, M. Matinmikko, J. Kalliovaara, J. Ojaniemi, J. Suutala, R. Ekman, R. Bacchus, and D. Roberson, "Spectrum occupancy measurements: A survey and use of interference maps," *IEEE Commun. Surveys Tuts.*, vol. 18, no. 4, pp. 2386–2414, 4th Quart., 2016.

[4] Q. Zhao and B. M. Sadler, "A survey of dynamic spectrum access," *IEEE Signal Process. Mag.*, vol. 24, no. 3, pp. 79–89, May 2007.

[5] R. H. Tehrani, S. Vahid, D. Triantafyllopoulou, H. Lee, and K. Moessner, "Licensed spectrum sharing schemes for mobile operators: A survey and outlook," *IEEE Commun. Surveys Tuts.*, vol. 18, no. 4, pp. 2591–2623, 4th Quart., 2016.

[6] A. B. Flores, R. E. Guerra, E. W. Knightly, P. Ecclesine, and S. Pandey, "IEEE 802.11af: A standard for TV white space spectrum sharing," *IEEE Commun. Mag.*, vol. 51, no. 10, pp. 92–100, Oct. 2013.

[7] M. M. Sohul, M. Yao, T. Yang, and J. H. Reed, "Spectrum access system for the citizen broadband radio service," *IEEE Commun. Mag.*, vol. 53, no. 7, pp. 18–25, Jul. 2015.

[8] T. Yucek and H. Arslan, "A survey of spectrum sensing algorithms for cognitive radio applications," *IEEE Commun. Surveys Tuts.*, vol. 11, no. 1, pp. 116–130, 1st Quart., 2009.

[9] G. Ding, J. Wang, Q. Wu, Y.-D. Yao, F. Song, and T. A. Tsiftsis, "Cellular-base-station-assisted device-to-device communications in TV white space," *IEEE J. Sel. Areas Commun.*, vol. 34, no. 1, pp. 107–121, Jan. 2016.

[10] K. Umebayashi, K. Moriwaki, R. Mizuchi, H. Iwata, S. Tiiro, J. J. Lehtomäki, M. López-Benítez, and Y. Suzuki, "Simple primary user signal area estimation for spectrum measurement," *IEICE Trans. Commun.*, vol. E99-B, no. 2, pp. 523–532, Feb. 2016.

[11] T. Fujii and K. Umebayashi, "Smart spectrum for future wireless world," *IEICE Trans. Commun.*, vol. E100-B, no. 9, pp. 1661–1673, Sep. 2017.

[12] J. J. Lehtomäki, M. López-Benítez, K. Umebayashi, and M. Juntti, "Improved channel occupancy rate estimation," *IEEE Trans. Commun.*, vol. 63, no. 3, pp. 643–654, Mar. 2015.

[13] K. Umebayashi, M. Kobayashi, and M. López-Benítez, "Efficient time domain deterministic-stochastic model of spectrum usage," *IEEE Trans. Wireless Commun.*, vol. 17, no. 3, pp. 1518–1527, Mar. 2018.

[14] T. Nguyen, B. L. Mark, and Y. Ephraim, "Spectrum sensing using a hidden bivariate Markov model," *IEEE Trans. Wireless Commun.*, vol. 12, no. 9, pp. 4582–4591, Sep. 2013.

[15] K. Umebayashi, K. Hayashi, and J. J. Lehtomäki, "Threshold-setting for spectrum sensing based on statistical information," *IEEE Commun. Lett.*, vol. 21, no. 7, pp. 1585–1588, Jul. 2017.

[16] K. Umebayashi, Y. Suzuki, and J. J. Lehtomäki, "Dynamic selection of CWmin in cognitive radio networks for protecting IEEE 802.11 primary users," in *Proc. 6th Int. ICST Conf. Cognit. Radio Oriented Wireless Netw. Commun.*, 2011, pp. 266–270.

[17] Y. Xu, A. Anpalagan, Q. Wu, L. Shen, Z. Gao, and J. Wang, "Decision-theoretic distributed channel selection for opportunistic spectrum access: Strategies, challenges and solutions," *IEEE Commun. Surveys Tuts.*, vol. 15, no. 4, pp. 1689–1713, 4th Quart., 2013.

[18] M. López-Benítez and F. Casadevall, "Methodological aspects of spectrum occupancy evaluation in the context of cognitive radio," *Eur. Trans. Telecommun.*, vol. 21, no. 8, pp. 680–693, Dec. 2010.

[19] A. Mariani, A. Giorgetti, and M. Chiani, "Effects of noise power estimation on energy detection for cognitive radio applications," *IEEE Trans. Commun.*, vol. 59, no. 12, pp. 3410–3420, Dec. 2011.

[20] R. Tandra and A. Sahai, "SNR walls for signal detection," *IEEE J. Sel. Topics Signal Process.*, vol. 2, no. 1, pp. 4–17, Feb. 2008.

[21] D. Torrieri, "The radiometer and its practical implementation," in *Proc. Mil. Commun. Conf. (MILCOM)*, Oct. 2010, pp. 304–310.

[22] A. Mariani, A. Giorgetti, and M. Chiani, "Robust detection with low-complexity SDRs: A pragmatic approach," in *Proc. IEEE 29th Annu. Int. Symp. Pers., Indoor Mobile Radio Commun. (PIMRC)*, Sep. 2018, pp. 1–6.

[23] H. Iwata, K. Umebayashi, A. Al-Tahmeesschi, M. López-Benítez, and J. Lehtomäki, "Time and frequency varying noise floor estimation for spectrum usage measurement," in *Proc. IEEE Wireless Commun. Netw. Conf. Workshop (WCNCW)*, Apr. 2019, pp. 1–6.

[24] M. Wellens, J. Wu, and P. Mähönen, "Evaluation of spectrum occupancy in indoor and outdoor scenario in the context of cognitive radio," in *Proc. IEEE CROWNCOM*, Aug. 2007, pp. 420–427.

[25] T. Harrold, R. Cepeda, and M. Beach, "Long-term measurements of spectrum occupancy characteristics," in *Proc. IEEE Int. Symp. Dyn. Spectr. Access Netw. (DySPAN)*, May 2011, pp. 83–89.

[26] J. Kokkoniemi and J. Lehtomäki, "Spectrum occupancy measurements and analysis methods on the 2.45 GHz ISM band," in *Proc. EAI CROWNCOM*, Jun. 2012, pp. 285–290.

[27] M. Ready, M. Downey, and L. Corbalis, "Automatic noise floor spectrum estimation in the presence of signals," in *Proc. IEEE ACSSC*, Nov. 1997, pp. 877–881.

[28] A. Agarwal, A. S. Sengar, and S. Debnath, "A novel noise floor estimation technique for optimized thresholding in spectrum sensing," in *Proc. Int. Conf. Adv. Comput., Commun. Informat. (ICACCI)*, Sep. 2017, pp. 607–611.

[29] J. Nikonowicz, A. Mahmood, and M. Gidlund, "A blind signal samples detection algorithm for accurate primary user traffic estimation," *Sensors*, vol. 20, no. 15, p. 4136, Jul. 2020.

[30] M. López-Benítez, J. Lehtomäki, K. Umebayashi, and D. Patel, "Accurate noise floor calibration based on modified expectation maximisation of Gaussian mixture," in *Proc. IEEE WCNC*, May 2019, pp. 1–6.

[31] J. Yao, M. Jin, Q. Guo, Y. Li, and J. Xi, "Effective energy detection for IoT systems against noise uncertainty at low SNR," *IEEE Internet Things J.*, vol. 6, no. 4, pp. 6165–6176, Aug. 2019.

[32] J. J. Lehtomäki, R. Vuohtoniemi, K. Umebayashi, and J.-P. Mäkelä, "Energy detection based estimation of channel occupancy rate with adaptive noise estimation," *IEICE Trans. Commun.*, vol. E95.B, no. 4, pp. 1076–1084, 2012.

[33] J. J. Lehtomäki, R. Vuohtoniemi, and K. Umebayashi, "On the measurement of duty cycle and channel occupancy rate," *IEEE J. Sel. Areas Commun.*, vol. 31, no. 11, pp. 2555–2565, Nov. 2013.

[34] H. Saarnisaari, P. Henttu, and M. Juntti, "Iterative multidimensional impulse detectors for communications based on the classical diagnostic methods," *IEEE Trans. Commun.*, vol. 53, no. 3, pp. 395–398, Mar. 2005.

[35] P. D. Welch, "The use of fast Fourier transform for the estimation of power spectra: A method based on time averaging over short, modified periodograms," *IEEE Trans. Audio Electroacoust.*, vol. AU-15, no. 2, pp. 70–73, Jun. 1967.

[36] N. Dinur and D. Wulich, "Peak-to-average power ratio in high-order OFDM," *IEEE Trans. Commun.*, vol. 49, no. 6, pp. 1063–1072, Jun. 2001.

[37] H. Ochiai and H. Imai, "On the distribution of the peak-to-average power ratio in OFDM signals," *IEEE Trans. Commun.*, vol. 49, no. 2, pp. 282–289, Feb. 2001.

[38] H. Iwata, K. Umebayashi, S. Tiiro, J. J. Lehtomäki, M. López-Benítez, and Y. Suzuki, "Welch FFT segment size selection method for spectrum awareness system," *IEICE Trans. Commun.*, vol. E99-B, no. 8, pp. 1813–1823, 2016.

[39] Z. Khan, J. J. Lehtomäki, E. Hossain, M. Latva-Aho, and A. Marshall, "An FPGA-based implementation of a multifunction environment sensing device for shared access with rotating radars," *IEEE Trans. Instrum. Meas.*, vol. 67, no. 11, pp. 2561–2578, Nov. 2018.

HIROKI IWATA (Member, IEEE) was born in Miyazaki, Japan, in 1992. He received the B.E., M.E., and Ph.D. degrees in electrical and electronic engineering from the Tokyo University of Agriculture and Technology, Tokyo, Japan, in 2014, 2016, and 2019, respectively. He was a Postdoctoral Researcher with the Tokyo University of Agriculture and Technology, from 2019 to 2021. He is currently working with the Research and Development Department, Hitachi Kokusai Electric Inc. His research interests include cognitive radio networks, spectrum measurement, and wireless communication systems. He received the Best Paper Award in the International Workshop on Smart Spectrum (IWSS) at IEEE WCNC 2016 for a paper he authored.

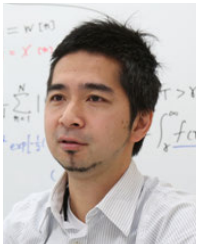

KENTA UMEBAYASHI (Member, IEEE) received the L.L.B. degree from Ritsumeikan University, Japan, in 1996, and the B.E., M.E., and Ph.D. degrees from Yokohama National University, Japan, in 1999, 2001, and 2004, respectively. From 2004 to 2006, he was a Research Scientist with the Centre for Wireless Communications, University of Oulu, Finland. He is currently a Professor with the Tokyo University of Agriculture and Technology, Japan. His research interests include the areas of signal detection and estimation theories for wireless communication, signal processing for multiple antenna systems, cognitive radio networks, and Terahertz band wireless communications. He was a Principal Investigator of four grants-in-aid for scientific research projects and three strategic information and communications research and development promotion programme projects, including a HORIZON2020 project. He received the Best Paper Award at 2012 IEEE WCNC and the Best Paper Award at 2015 IEEE WCNC Workshop from IWSS.

AHMED AL-TAHMEESSCHI (Member, IEEE) received the B.Sc. and M.Sc. degrees in communications engineering from the University of Technology, Baghdad, Iraq, in 2009 and 2011, respectively, and the Ph.D. degree from the Department of Electrical Engineering and Electronics, University of Liverpool, U.K., in 2018. He is currently a Postdoctoral Researcher with the Tokyo University of Agriculture and Technology. His research interests include cognitive radio networks, dynamic spectrum access techniques, algorithm design, and machine learning.

JANNE LEHTOMÄKI (Member, IEEE) received the Ph.D. degree from the University of Oulu, Oulu, Finland, in 2005. He is currently an Adjunct Professor (docent) with the Centre for Wireless Communications, University of Oulu. He spent the fall 2013 semester at Georgia Tech, Atlanta, as a Visiting Scholar. He is currently focusing on cognitive radios and terahertz band wireless communication. He coauthored the paper receiving the Best Paper Award at IEEE WCNC 2012. He is an Associate Editor of *Physical Communication*.